

Presumed Müller Cell Activation in Multiple Evanescent White Dot Syndrome

Maria Vittoria Cicinelli¹ ,² Matteo Menean,¹ Aurelio Apuzzo,¹ Pierluigi Scandale,¹ Alessandro Marchese,¹ Ugo Introini,¹ Maurizio Battaglia Parodi,¹ Francesco Bandello,¹ and Elisabetta Misericocchi¹

¹School of Medicine, Vita-Salute San Raffaele University, Milan, Italy

²Department of Ophthalmology, IRCCS San Raffaele Scientific Institute, Milan, Italy

Correspondence: Maria Vittoria Cicinelli, Department of Ophthalmology, IRCCS San Raffaele Scientific Institute, Via Olgettina 60, Milan 20132, Italy; cicinelli.mariavittoria@hsr.it.

Received: May 29, 2023

Accepted: September 20, 2023

Published: October 12, 2023

Citation: Cicinelli MV, Menean M, Apuzzo A, et al. Presumed Müller cell activation in multiple evanescent white dot syndrome. *Invest Ophthalmol Vis Sci.* 2023;64(13):20. <https://doi.org/10.1167/iovs.64.13.20>

PURPOSE. The purpose of this study was to investigate the foveal changes occurring in multiple evanescent white dot syndrome (MEWDS) using multimodal imaging techniques with a specific focus on hyper-reflective dots (HRDs).

METHODS. This was a retro-prospective observational study including 35 eyes with active MEWDS. Structural and en face optical coherence tomography (OCT) was performed, with follow-up visits at 2 weeks, 6 weeks, and 2 months from baseline. HRD percentage area (HRD % area) was calculated in a 600 μm fovea centered circle on en face OCT, after background subtraction and image binarization. HRD % area was compared with 23 fellow control eyes. Longitudinal changes in the HRD % areas were assessed using repeated-measure statistics.

RESULTS. HRDs were observed as scattered hyper-reflective spots on the vitreoretinal interface on en face OCT images, colocalizing with HRDs or vertical hyper-reflective lines on structural OCT images. The baseline evaluation showed a significantly higher HRD % area in MEWDS eyes compared to fellow eyes (0.10 ± 0.03 vs. 0.08 ± 0.04 , $P = 0.01$). The HRD % area correlated positively with LogMAR visual acuity and inversely with the duration of symptoms. Longitudinal analysis revealed a significant reduction in the HRD % area over time. There was no significant interaction between the rate of HRD disappearance and clinical or demographic factors at baseline.

CONCLUSIONS. As HRD potentially represents the end-feet projections of activated Müller cells on the retinal surface, this study supports the involvement of Müller cells in the pathogenesis of the disease. The findings highlight the potential of en face OCT imaging for monitoring the progression of MEWDS.

Keywords: multiple evanescent white dot syndrome (MEWDS), white dot syndromes, en face optical coherence tomography (OCT), Müller cells

Multiple evanescent white dot syndrome (MEWDS), first described by Jampol et al. in 1983, is an inflammatory disease primarily affecting the outer retina. It typically manifests as unilateral, although rarely bilateral, and commonly affects young to middle-aged female patients. Classic symptoms include acute blurred vision, photopsia, and enlargement of the blind spot. Multimodal imaging (MMI) techniques have greatly enhanced our understanding of the pathogenesis and clinical manifestations of MEWDS.^{1,2}

Previous studies have established that MEWDS primarily involves the outer retina, causing reversible disruption of the photoreceptors' outer segments.³ Spectral-domain optical coherence tomography (SD-OCT) has revealed focal interruptions in the ellipsoid zone (EZ) and interdigitation zone (IZ) bands, corresponding to the "spots" observed in other imaging modalities.³ In addition, SD-OCT imaging at the fovea may exhibit variable-sized and shaped vertical hyper-reflective lesions, which have yet to be univocally characterized.⁴⁻⁶

En face optical coherence tomography (OCT) is a noninvasive technology that provides high-resolution, cross-sectional images of the retina. En face OCT offers a distinct advantage by enabling visualization of retinal layers in the en face plane, parallel to the retinal surface. This unique capability allows for a comprehensive assessment of the extent and distribution of retinal abnormalities in vascular, degenerative, and inflammatory diseases.^{7,8} In recent studies, en face OCT has shown foveal hyper-reflective dots (HRDs) on the retinal surface of both healthy and diseased eyes.^{9,10} HRDs have been interpreted as the projections of Müller cells' end-feet over the internal limiting membrane (ILM),¹¹ paving the way for the role of Müller cells in the structural organization of the fovea and their potential involvement in retinal pathologies.

To further elucidate the foveal changes occurring in MEWDS and provide a plausible explanation for the MMI findings, we longitudinally investigated the vitreoretinal interface during the acute and resolving phases of this



disease, with a particular focus on HRDs. We hypothesized foveal Müller cells' involvement in active MEWDS, possibly correlating with demographic and clinical findings at the onset of the disease.

METHODS

This was a retrospective, prospective, observational study conducted at the Department of Ophthalmology of the San Raffaele Scientific Institute in Milan, Italy, between 2014 and 2023. The study adhered to the guidelines outlined in the Health Insurance Portability and Accountability Act of 1996 and followed the principles of the Declaration of Helsinki. Ethical approval was obtained from the local ethics committee.

The study included patients with clinical and imaging features consistent with active MEWDS.⁴ Patients with incomplete demographic and clinical data, those without available en face SD-OCT scans for review, and those with systemic or ocular diseases that mimicked MEWDS (such as syphilis, vitreoretinal lymphoma, or autoimmune retinopathy) were excluded. Patients with ocular conditions that could affect en face SD-OCT analysis (such as epiretinal membrane, lamellar hole, or vitreous opacity) and those with OCT motion artifacts were also excluded. Furthermore, patients were categorized into primary or secondary MEWDS based on other clinical conditions that presumably triggered the inflammatory reaction.^{12,13} The fellow eye was included as the control if healthy.

The first visit where active MEWDS was diagnosed was considered the baseline for this study. Follow-up visits were scheduled at 2 weeks, 6 weeks, and 2 months from the baseline visit. Data collection at each visit included ocular history, measurement of LogMAR visual acuity, refraction assessment, slit-lamp examination, and MMI. For each eye, time (days) from symptoms onset, foveal involvement (identified as subfoveal EZ/IZ disruption), and presence of foveal vertical hyper-reflective lesions on SD-OCT was recorded.⁴⁻⁶

Imaging Protocol and Analysis

All patients underwent SD-OCT (Spectralis HRA + OCT; Heidelberg Engineering, Heidelberg, Germany) using a volume protocol of 131 B-scans, each with a thickness of 11 μ m, covering the macular area of 15 degrees \times 5 degrees. Structural SD-OCT scans were obtained by averaging 25 SD-OCT B-scans. En face SD-OCT images were acquired using the built-in software (Spectralis; Heidelberg Engineering), focusing on the slab between the ILM and ILM +3 μ m. This specific slab was chosen to optimize the visualization of HRD.

All SD-OCT en face slabs, both with and without foveal cross-markers, were exported as JPEG files into ImageJ (National Institutes of Health, Bethesda, MD). A manually selected fovea-centered circle with a diameter of 600 μ m was chosen as the region of interest (ROI), which anatomically corresponded to the average size of the foveal avascular zone in healthy subjects (Supplementary Fig. S1A).¹⁴ The Analyze -> Histogram tool was used to calculate the modal pixel intensity within the ROI. The mode was chosen to account for any skewness in non-normal distributions of pixel intensities. The modal pixel intensity was then subtracted from the ROI to flatten the background and enhance hyper-reflective lesions (Supplementary Fig. S1B).

The Process -> Find maxima function was used to create a binary (mask-like) image of the lesions that stood out from the surrounding background by more than one standard deviation (SD) from the average pixel intensity of the ROI. These lesions were considered HRD. The Analyze -> Analyze Particle tool was employed to calculate the percentage area (% area) of these lesions with respect to the ROI (Supplementary Fig. S1C). In order to assess the robustness of our method and validate our findings, we conducted an additional binarization of each image, considering HRD as lesions with a pixel intensity of 2 SDs above the mean pixel intensity of the ROI.

Statistical Analysis

Statistical calculations were performed using the R program (version 4.1.2). Demographic and clinical differences between primary MEWDS and secondary MEWDS were summarized as mean \pm SD.

The first outcome of the study was to compare the % area of HRD at baseline between MEWDS eyes and fellow control eyes. We used a generalized linear model (GLM) that included the patient identification number as a random effect to account for intrasubject correlations. The secondary outcome aimed to correlate the HRD % area in the study eyes with the demographic and clinical features of each patient. Pearson's correlation coefficients and *P* values were provided for significant associations.

The tertiary outcome involved assessing the longitudinal change in the HRD % area in MEWDS eyes. We utilized a repeated-measure GLM that included clinical characteristics and their interaction with time as fixed covariates, and the eye identification number as a random effect. Significance levels of alpha 0.05 and 0.1 were reported.

RESULTS

A total of 35 eyes of 34 patients were included in the study. The mean age of the patients was 36.8 \pm 14 years, ranging from 17 to 65. Out of the 34 patients, 25 were women (74%). All patients presented with acute symptoms, such as visual loss, floaters, or photopsia. The average time between the onset of symptoms and the first visit was 10 \pm 8.6 days, ranging from 1 to 30 days. To serve as controls, 23 healthy fellow eyes were also included.

Twenty eyes of 19 patients (57%) had primary MEWDS, whereas 15 eyes of 15 patients (43%) had secondary MEWDS. Among those with secondary MEWDS, 14 patients had idiopathic multifocal choroiditis, and 1 patient had angioid streaks. Patients with primary MEWDS were younger, with a mean age of 29.2 \pm 9.90 years, compared to those with secondary MEWDS (48.4 \pm 12.1 years). Additionally, patients with primary MEWDS had less severe myopic refraction (-0.86 \pm 2.45 D) and higher choroidal thickness (381 \pm 83.2 μ m) compared to those with secondary MEWDS (-6.63 \pm 3.51 D and 189 \pm 110 μ m, respectively; see the Table). The primary MEWDS group more frequently exhibited foveal involvement (90% vs. 40%) and foveal vertical hyper-reflective lines on structural SD-OCT (60% vs. 33%). However, the visual acuity at the baseline visit was similar between the two groups.

Two patients with primary MEWDS received treatment with oral corticosteroids. All patients with secondary

TABLE. Demographic and Clinical Characteristics of Patients Stratified Into Primary and Secondary MEWDS.

	Primary MEWDS (N = 20)	Secondary MEWDS (N = 15)	Overall (N = 35)
Age, y)			
Mean (SD)	29.2 (9.90)	48.4 (12.1)	37.1 (14.4)
Median [Min, Max]	26.5 [17.0, 52.0]	51.0 [28.0, 65.0]	36.0 [17.0, 65.0]
Female gender	15 (75.0%)	10 (66.7%)	25 (71.4%)
Foveal involvement	18 (90.0%)	6 (40.0%)	24 (68.6%)
Choroidal thickness (µm)			
Mean (SD)	381 (83.2)	189 (110)	302 (134)
Median [Min, Max]	361 [204, 528]	173 [56.0, 380]	326 [56.0, 528]
Vertical hyper-reflective lines	12 (60.0%)	5 (33.3%)	17 (48.6%)
Refraction (diopters)			
Mean (SD)	-0.86 (2.45)	-6.63 (3.51)	-3.13 (4.04)
Median [Min, Max]	0.225 [-5.30, 3.00]	-7.00 [-14.0, -2.00]	-2.00 [-14.0, 3.00]
Visual acuity (LogMAR)			
Mean (SD)	0.28 (0.25)	0.33 (0.31)	0.30 (0.27)
Median [Min, Max]	0.25 [0, 1.00]	0.20 [0, 1.00]	0.20 [0, 1.00]

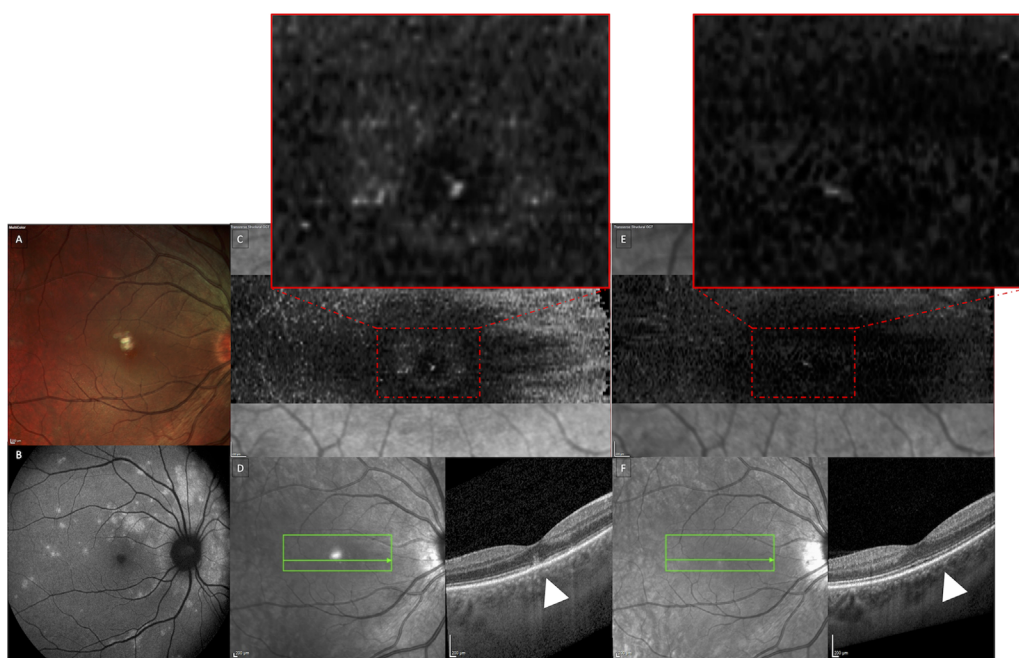


FIGURE 1. Longitudinal foveal changes in a patient with primary multiple evanescent white dot syndrome (MEWDS). (A) Fundus multicolor imaging reveals the presence of multiple whitish dots distributed around the optic disc and posterior pole. (B) Blue-light fundus autofluorescence (BAF) demonstrates multiple areas of hyper-autofluorescence corresponding to the white dots on multicolor imaging. (C) En face OCT (slab between ILM and ILM +3 µm) at baseline exhibits numerous perifoveal hyper-reflective dots (HRD) measuring 10 to 12 µm in size. (D) Structural OCT reveals disruption of the ellipsoid zone (EZ) and interdigitation zone (IZ), with vertical hyper-reflective lesions protruding toward the inner retina. (E) En face OCT (slab between ILM and ILM +3 µm) at 6 weeks demonstrates a reduction in the number of HRDs. (F) Structural OCT shows complete restoration of the EZ/IZ under the fovea and disappearance of the vertical hyper-reflective lesions.

MEWDS were treated with either corticosteroids or systemic immunosuppression.

Baseline HRD Evaluation

HRD appeared as scattered hyper-reflective spots measuring 10 to 30 µm at the vitreoretinal interface, forming small clusters around the central fovea (Figs. 1–3). We observed statistically significant differences between the study and fellow eyes when considering a pixel intensity threshold of 2 SDs above the mean intensity of the ROI in the HRD selection process (0.045 ± 0.028 vs. 0.027 ± 0.02 , $P = 0.02$).

We observed a distinctive pattern in acute MEWDS, characterized by vertical hyper-reflective material originating from the outer retinal bands and extending toward the inner retina. These vertical lines were positioned at the foveal center and coincided with focal defects in the EZ/IZ. Below the vertical lines, a thin area of choroidal hypertransmission was present. Although most cases featured solitary vertical lines, some exhibited additional adjacent lesions. These lesions varied in appearance, with some spanning from the outer to inner retina, whereas others did not reach the inner retinal surface (Supplementary Fig. S2). Furthermore, some lesions formed continuous lines, whereas others displayed a fragmented appearance. At the termination of these lines,

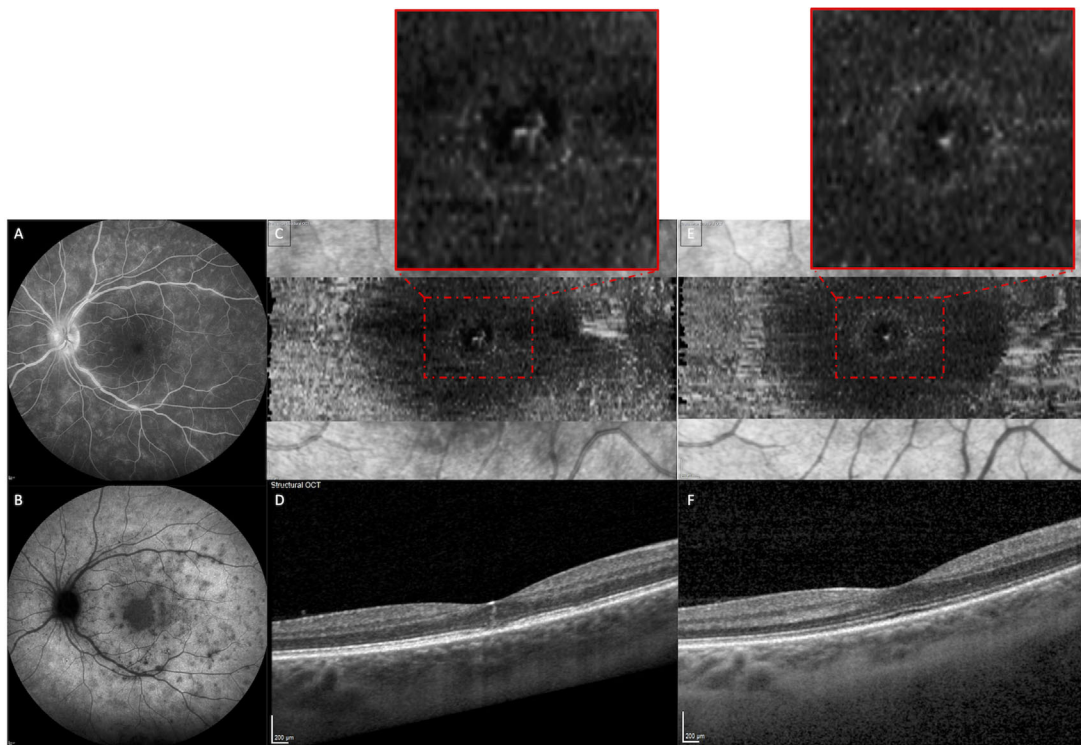


FIGURE 2. Longitudinal foveal changes in a patient with primary multiple evanescent white dot syndrome (MEWDS). (A) Fundus fluorescein angiography reveals mild optic nerve and large vessel leakage, accompanied by wreath-like hyper-reflective lesions at the posterior pole. (B) Indocyanine green angiography displays hypofluorescent dots and spots in the late frames of the examination. (C) En face OCT (slab between ILM and ILM +3 μ m) at baseline demonstrates multiple perifoveal hyper-reflective dots (HRDs) measuring 10 to 12 μ m in size, occasionally merging together. (D) Structural OCT shows disruption of the ellipsoid zone (EZ) and interdigitation zone (IZ) at the fovea, along with a vertical hyper-reflective lesion extending from the EZ/IZ to the internal limiting membrane (ILM), terminating with an intense hyper-reflective lesion resting on the retinal surface. (E) En face OCT (slab between ILM and ILM +3 μ m) at 8 weeks exhibits a decrease in the number of HRDs. (F) Structural OCT demonstrates complete restoration of the EZ/IZ beneath the fovea and disappearance of the vertical hyper-reflective lesion.

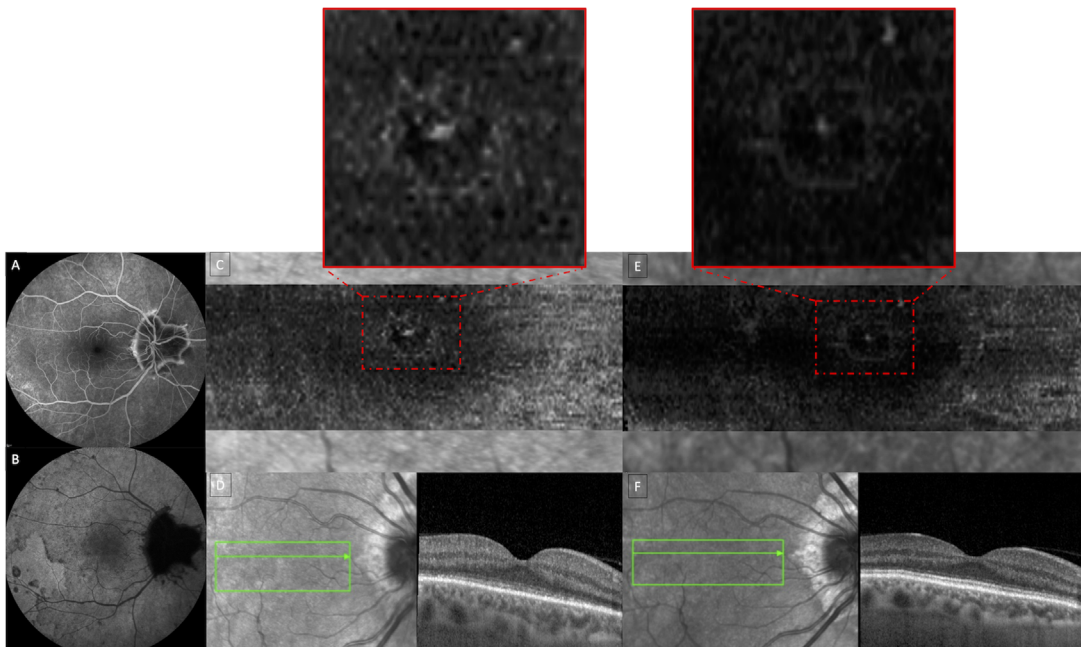


FIGURE 3. Longitudinal foveal changes in a patient with multiple evanescent white dot syndrome (MEWDS) secondary to angioid streaks. (A) Fundus fluorescein angiography (FA) displays peripapillary hypofluorescence corresponding to retinal pigment epithelium (RPE) atrophy, with hyper-reflective staining along the borders. (B) Indocyanine green angiography reveals an extensive, merging region of hypofluorescence with discrete spots in the temporal macula. (C) En face OCT (slab between ILM and ILM +3 μ m) reveals multiple hyper-reflective dots (HRDs) surrounding the foveal depression. (D) Structural OCT demonstrates diffuse attenuation of the ellipsoid zone (EZ) and interdigitation zone (IZ). (E, F) Follow-up imaging exhibits a decrease in the number of HRDs on en face OCT and complete restoration of the EZ/IZ bands on structural OCT.

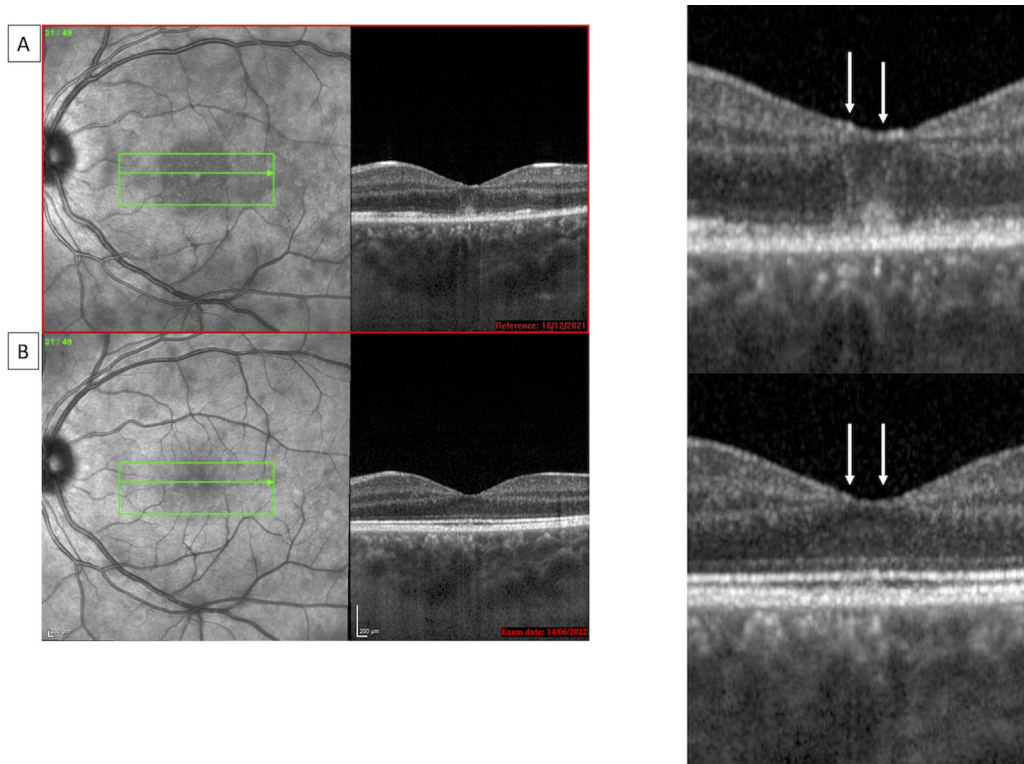


FIGURE 4. Resolution of foveal lesions in a patient with multiple evanescent white dot syndrome (MEWDS). (A) Structural OCT of a patient with active MEWDS reveals disruption of the ellipsoid zone (EZ) and interdigitation zone (IZ) bands beneath the fovea, accompanied by hyper-reflective vertical lesions extending from the EZ/IZ to the inner limiting membrane. The hyper-reflective vertical lesions conclude with small, elevated dots of intense reflectivity on the retinal surface. (B) Structural OCT of the same patient, obtained during the resolution phase of MEWDS using a follow-up mode. The OCT scan demonstrates the resolution of the outer retinal lesion and the disappearance of hyper-reflective dots on the vitreoretinal interface.

a slightly elevated punctiform hyper-reflective lesion was observed, situated on the vitreoretinal interface (Fig. 4). Multidimensional reconstructions (Supplementary Fig. S3) provided additional confirmation of the co-localization of HRD on en face images with the vertical lines detected on structural OCT.

In the study eyes, a positive correlation was found between the HRD % area and LogMAR visual acuity ($r = 0.33$,

$P = 0.07$), indicating that a larger HRD % area was associated with worse visual acuity. Conversely, an inverse correlation was observed between the HRD % area and the number of days elapsed since the onset of symptoms ($r = -0.35$, $P = 0.04$), suggesting that the HRD % area decreased as time progressed. No significant difference was seen in HRD % area between primary and secondary MEWDS ($P = 0.9$).

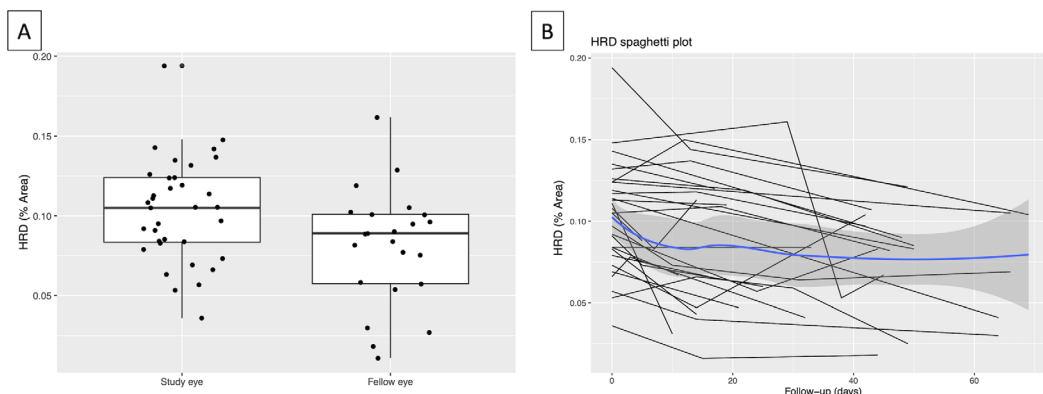


FIGURE 5. Quantitative analysis of hyper-reflective dots (HRD) percentage area (% area) at baseline and during follow-up. (A) Box plot graph illustrating the relative area of HRD within a 600- μ m region of interest (ROI) centered on the fovea. HRD are considered as binarized lesions that stood out from the surrounding background by more than one standard deviation from the average pixel intensity of the ROI. Given that our sample size is relatively small, we showed all the data as black dots. Eyes affected by multiple evanescent white dot syndrome (MEWDS) exhibit a significantly larger HRD % area compared to fellow healthy eyes. (B) Normalized changes in HRD % area over time in patients with MEWDS. Each curve represents an individual patient, with HRD area normalized to 1.0 at the study's onset. There was a noticeable reduction in HRD area, particularly in the initial 15 days.

Longitudinal HRD Evaluation

Six eyes had a baseline visit only and were excluded by the longitudinal evaluation. The remaining 29 eyes had a mean follow-up period of 42.3 ± 18.4 days, ranging from 5 to 69. The mean HRD % area was significantly higher in eyes affected by MEWDS compared to fellow eyes (0.10 ± 0.03 vs. 0.08 ± 0.04 , $P = 0.01$; Fig. 5A). Over time, there was a significant reduction in the HRD % area, from 0.10 ± 0.03 to 0.07 ± 0.03 ($P < 0.001$; Fig. 5B). The reduction in HRD % area paralleled normalization of the outer retina, disappearance of vertical lines, and improvement in visual acuity.

At the last visit, the HRD % area was comparable between the study and fellow eyes ($P = 0.4$). There was a significant interaction between time and foveal involvement ($P = 0.02$), suggesting a faster reduction of HRD % area in eyes with no foveal involvement. No significant interaction was observed between the rate of HRD disappearance and the demographic factors at the baseline (Supplementary Table S1).

DISCUSSION

En face OCT imaging has greatly advanced our understanding of retinal diseases, including MEWDS. Longitudinal studies tracked the evolution and resolution of the characteristic dots and spots, providing essential information on disease progression and prognosis.^{3,15,16} This study focuses on the vitreoretinal interface in patients with MEWDS, aiming to monitor the foveal changes occurring during different phases of the disease. We observed the presence of multiple discrete HRD on the central foveal surface of patients with MEWDS, which were more abundant compared to control eyes. The % area of HRD was found to be higher in eyes with worse initial visual acuity, peaking during the acute phase of the disease and gradually decreasing over a 2-month period.

The human fovea is known for its high concentration of Müller cells, which support neuronal function, regulate retinal blood flow, maintain ion and water balance, and modulate immune and inflammatory responses.^{17,18} The central fovea also contains specialized Müller cell cones that extend from the external limiting membrane to the floor of the foveal pit and terminate with horizontal processes under the ILM.¹⁹

Müller cells undergo adaptive changes in response to traumatic, inflammatory, or ischemic stimuli.^{20–22} Notably, a specific group of structural proteins known as intermediate filaments, including vimentin and glial fibrillary acidic protein (GFAP), are upregulated in mice and porcine Müller cells in response to retinal injury.^{21,23} These proteins serve as stress markers in astrocytes of the central nervous system. Müller cells also become thicker and acquire a more branched cellular structure, leading to cell hypertrophy. Previous studies utilizing electron microscopy,²⁴ histopathology,¹¹ and in vivo imaging examinations^{9,10} have demonstrated that activated Müller cells can be visualized as aggregated white granules, typically ranging from 5 to 20 μm in diameter, with multiple protrusions and cilia-like structures along the slope of the foveal depression. Consistent with previous findings, we hypothesize that the increase in HRD % area in active MEWDS reflects functional and structural transformations in activated Müller cells. The correlation between HRD % area and presenting visual acuity further

emphasizes their potential as biomarkers for disease severity and visual prognosis.

Twenty-nine eyes were followed up for an average of 6 weeks. Over time, there was a significant reduction in the HRD % area, that paralleled the resolution of the outer retinal lesions typical of MEWDS. The disappearance of HRD supports the idea that HRD reflect an acute inflammatory response that resolves with disease regression. Interestingly, there was a significant interaction between time and foveal involvement, indicating a faster reduction of HRD % area in eyes with extrafoveal lesions. On the other hand, the absence of interactions with demographic factors suggests that HRD dynamics are consistent across different patient profiles.

This study also noted the presence of vertical hyper-reflective lines in the central fovea of 17 eyes. These lines, originating from the RPE and extending vertically or curvilinearly toward the inner retina, have been observed in degenerative diseases, tractional maculopathies, and inflammatory conditions.^{5,25} Dolz-Marco described three patients with active idiopathic multifocal choroiditis with foveal outer retinal hyper-reflectivity extending from the EZ to the inner portion of the ONL.⁶ Marsiglia et al.⁴ and Ramthoul et al.²⁶ reported foveal lesions with a columnar appearance overlying acute photoreceptors disruption; similar findings were included in a case series by Amoroso et al.⁵ The absence of clear backscattering and the disappearance of the lesions without leaving any legacy made the possibility of these lines being pigmented cells from damaged retinal pigment epithelium unlikely. Additionally, no perifoveal radial pattern of vertical lines suggesting photoreceptors debris aligning Henle fibers has been observed in the examined eyes.

Notably, vertical hyper-reflective lines tended to be transient and disappeared as inflammation subsided. We speculate that these lines depict temporary changes in the optical reflectivity of central Müller cells. In fact, the biological and architectural transformations have the potential to influence Müller cells' optical properties²⁷ and may contribute to increased hyper-reflectivity when imaged using OCT. Although there was no direct correlation between the presence of vertical hyper-reflective lines and the extent of HRD, the two lesions tended to colocalize on structural OCT scans. Thus, we propose that vertical hyper-reflective lines and HRD both represent two indirect signs of Müller cell activation, with one visualized on structural OCT and the other on en face reconstructions.

It is important to acknowledge the limitations of this study. First, the sample size was relatively small, which may restrict the generalizability of our findings; although 35 cases could certainly limit the results of the study in terms of statistical power, MEWDS is a rare disease and larger cohorts of patients have been rarely presented in the literature. Additionally, the varying follow-up periods among patients could introduce variability in the longitudinal evaluation. Although our study aimed to establish an association between HRD and Müller cell activation in MEWDS, we recognize that HRD may not be exclusive to this condition. HRD could potentially represent other pathological features, such as macrophage-like cells found along large retinal blood vessels and may not be uniquely related to vertical hyper-reflective lines.^{28,29}

We took measures to enhance reproducibility and accuracy by using a semi-automated method for visualizing and quantifying HRD. We focused our analysis on the foveal area, where HRD were most clearly visualized, and did not

extend it to the adjacent macular regions. Furthermore, we performed a sensitivity analysis, using 2 SDs as a binarization threshold for HRD. However, we are aware that proper visualization of HRD can be challenging due to factors like slab thickness, light-reflex artifacts, vitreous opacities, and individual anatomical characteristics.⁹ We fully acknowledge the need for further validation through larger sample sizes and the utilization of advanced high-resolution imaging modalities or artificial intelligence algorithms approaches. Additionally, collaborative research and investigations that compare HRD with other pathological entities will be instrumental in strengthening the reliability and specificity of HRD as a potential biomarker.

In conclusion, this study contributes to our understanding of the retinal changes associated with MEWDS. The presence of HRD and their presumed association with Müller cell activation provide insights into the pathophysiology of the disease and potential biomarkers for disease progression. Future studies can build upon these findings to explore the underlying mechanisms of HRD formation and resolution, as well as the clinical implications of Müller cell activation in MEWDS and other retinal diseases.

Acknowledgments

This research did not receive any specific grant from funding agencies in the public, commercial, or not-for-profit sectors.

Competing Interests Statement: The authors have no competing interest in publishing the present work.

Contributorship Statement: All the authors contributed to the conception or design of the work, the acquisition, analysis, and interpretation of data, drafting of the work, and revising it critically for intellectual content. Each of the coauthors has seen and agrees with the way his or her name is listed.

Disclosure: M.V. Cicinelli, None; M. Menean, None; A. Apuzzo, None; P. Scandale, None; A. Marchese, None; U. Introini, None; M. Battaglia Parodi, None; F. Bandello, Allergan Inc., Irvine, CA, USA (C), Bayer Shering-Pharma, Berlin, Germany (C), Hoffmann-La-Roche, Basel, Switzerland (C), Novartis, Basel, Switzerland (C), Sanofi-Aventis, Paris, France (C), Thrombogenics, Heverlee, Belgium (C), Zeiss, Dublin, USA (C), Boehringer-Ingelheim (C), Fidia Sooft (C), Ntc Pharma (C), Sifi (C); E. Miserocchi, None

References

- Gargouri MA, Yousfi N, Toutain J, et al. Multiple evanescent white dot syndrome following COVID-19 mRNA vaccination. *Ocul Immunol Inflamm*. 2022;31(6):1240–1244.
- Baglivo E, Safran AB, Borruat FX. Multiple evanescent white dot syndrome after hepatitis B vaccine. *Am J Ophthalmol*. 1996;122(3):431–432.
- Pichi F, Srivastava SK, Chexal S, et al. En face optical coherence tomography and optical coherence tomography angiography of multiple evanescent white dot syndrome: new insights into pathogenesis. *Retina*. 2016;36(Suppl 1):S178–S188.
- Marsiglia M, Gallego-Pinazo R, Cunha de Souza E, et al. Expanded clinical spectrum of multiple evanescent white dot syndrome with multimodal imaging. *Retina*. 2016;36(1):64–74.
- Amoroso F, Mrejen S, Pedinielli A, et al. Intraretinal hyperreflective lines. *Retina*. 2021;41(1):82–92.
- Dolz-Marco R, Kalevar A, McDonald HR, et al. Foveal outer retinal hyperreflectivity: a novel optical coherence tomography finding in idiopathic multifocal choroiditis. *Retin Cases Brief Rep*. 2021;15(6):651–656.
- Rosen RB, Hathaway M, Rogers J, et al. Multidimensional en-face OCT imaging of the retina. *Opt Express*. 2009;17(5):4112–4133.
- Ghasemi Falavarjani K, Phasukkijwatana N, Freund KB, et al. En face optical coherence tomography analysis to assess the spectrum of perivenular ischemia and paracentral acute middle maculopathy in retinal vein occlusion. *Am J Ophthalmol*. 2017;177:131–138.
- Corradetti G, Au A, Borrelli E, et al. Analysis of hyperreflective dots within the central fovea in healthy eyes using en face optical coherence tomography. *Invest Ophthalmol Vis Sci*. 2019;60(13):4451–4461.
- Pole C, Au A, Navajas E, et al. En face optical coherence tomography imaging of foveal dots in eyes with posterior vitreous detachment or internal limiting membrane peeling. *Invest Ophthalmol Vis Sci*. 2021;62(10):5.
- Yokotsuka K, Kishi S, Shimizu K. White dot fovea. *Am J Ophthalmol*. 1997;123(1):76–83.
- Cicinelli MV, Hassan OM, Gill MK, et al. A multiple evanescent white dot syndrome-like reaction to concurrent retinal insults. *Ophthalmol Retina*. 2020;5(10):1017–1026.
- Essilfie J, Bacci T, Abdelhakim AH, et al. Are there two forms of multiple evanescent white dot syndrome? *Retina*. 2022;42(2):227–235.
- John D, Kuriakose T, Devasahayam S, Braganza A. Dimensions of the foveal avascular zone using the Heidelberg retinal angiogram-2 in normal eyes. *Indian J Ophthalmol*. 2011;59(1):9–11.
- De Bats F, Wolff B, Vasseur V, et al. “En-face” spectral-domain optical coherence tomography findings in multiple evanescent white dot syndrome. *J Ophthalmol*. 2014;2014:928028.
- Su D, Xu D, Phasukkijwatana N, Sarraf D. En face optical coherence tomography of multiple evanescent white dot syndrome. *Retin Cases Brief Rep*. 2017;11(Suppl 1):S121–S123.
- Ramtohil P, Cabral D, Sadda S, et al. The OCT angular sign of Henle fiber layer (HFL) hyperreflectivity (ASHH) and the pathoanatomy of the HFL in macular disease. *Prog Retin Eye Res*. 2022;95(2023):101135.
- Bringmann A, Pannicke T, Grosche J, et al. Müller cells in the healthy and diseased retina. *Prog Retin Eye Res*. 2006;25(4):397–424.
- Gass JD. Müller cell cone, an overlooked part of the anatomy of the fovea centralis: hypotheses concerning its role in the pathogenesis of macular hole and foveomacular retinoschisis. *Arch Ophthalmol*. 1999;117(6):821–823.
- Dyer MA, Cepko CL. Control of Müller glial cell proliferation and activation following retinal injury. *Nat Neurosci*. 2000;3(9):873–880.
- Wurm A, Iandiev I, Uhlmann S, et al. Effects of ischemia-reperfusion on physiological properties of Müller glial cells in the porcine retina. *Invest Ophthalmol Vis Sci*. 2011;52(6):3360–3367.
- Lindqvist N, Liu Q, Zajadacz J, et al. Retinal glial (Müller) cells: sensing and responding to tissue stretch. *Invest Ophthalmol Vis Sci*. 2010;51(3):1683–1690.
- Lewis GP, Fisher SK. Up-regulation of glial fibrillary acidic protein in response to retinal injury: its potential role in glial remodeling and a comparison to vimentin expression. *Int Rev Cytol*. 2003;230:263–290.
- Syrbe S, Kuhrt H, Gartner U, et al. Müller glial cells of the primate foveola: an electron microscopical study. *Exp Eye Res*. 2018;167:110–117.

25. Scharf JM, Hilely A, Preti RC, et al. Hyperreflective stress lines and macular holes. *Invest Ophthalmol Vis Sci.* 2020;61(4):50.
26. Ramtohul P, Gascon P, Denis D. Outer retinal plume signature in multiple evanescent white dot syndrome. *Ophthalmol Retina.* 2020;4(8):766.
27. Mat Nor MN, Guo CX, Green CR, et al. Hyper-reflective dots in optical coherence tomography imaging and inflammation markers in diabetic retinopathy. *J Anat.* 2023;243:697–705.
28. Castanos MV, Zhou DB, Linderman RE, et al. Imaging of macrophage-like cells in living human retina using clinical OCT. *Invest Ophthalmol Vis Sci.* 2020;61(6):48.
29. Ong JX, Nesper PL, Fawzi AA, et al. Macrophage-like cell density is increased in proliferative diabetic retinopathy characterized by optical coherence tomography angiography. *Invest Ophthalmol Vis Sci.* 2021;62(10):2.